Two-color laser wavelength effect on intense terahertz generation in air*

Shufen Li(李淑芬)[1,2], Chenhui Lu(卢晨晖)[3,†], Chengshuai Yang(杨承帅)[2], Yanzhong Yu(余燕忠)[1], Zhenrong Sun(孙真荣)[2], and Shian Zhang(张诗按)[2,4,‡]

[1] *College of Physics and Information Engineering and Key Laboratory of Information Functional Material for Fujian Higher Education, Quanzhou Normal University, Quanzhou* 362000, *China*

[2] *State Key Laboratory of Precision Spectroscopy, and School of Physics and Materials Science, East China Normal University, Shanghai* 200062, *China*

[3] *College of Mechanical Engineering, Shanghai University of Engineering Science, Shanghai* 201620, *China*

[4] *Collaborative Innovation Center of Extreme Optics, Shanxi University, Taiyuan* 030006, *China*

(Received 26 February 2017; revised manuscript received 30 May 2017; published online 30 September 2017)

Near-IR femtosecond lasers have been proposed to produce high-field terahertz radiation in the air via the laser–plasma interaction, but the physical mechanism still needs to be further explored. In this work, we theoretically investigate the effect of the two-color laser wavelength on the terahertz generation in the air based on a transient photocurrent model. We show that the long wavelength laser excitation can greatly enhance the terahertz amplitude for a given total laser intensity. Furthermore, we utilize a local current model to illustrate the enhancement mechanism. Our analysis shows that the terahertz amplitude is determined by the superposition of contributions from individual ionization events, and for the long wavelength laser excitation, the electron production concentrates in a few ionization events and acquires the larger drift velocities, which results in the stronger terahertz radiation generation. These results will be very helpful for understanding the terahertz generation process and optimizing the terahertz output.

Keywords: THz generation, two-color scheme, laser–plasma interaction, near-IR laser simulation

PACS: 42.65.Re, 32.80.Fb, 52.50.Jm **DOI:** 10.1088/1674-1056/26/11/114206

1. Introduction

The high-field terahertz (THz) pulse has attracted considerable attention not only for the related applications,[1–6] such as remote sensing,[6] but also for the study of light–plasma interaction.[7–9] However, the high peak intensity THz pulse generation is still a major challenge in THz research. The traditional solution is based on optical rectification in nonlinear crystals;[10–12] this technique currently can deliver a THz pulse with GV/m electric field intensity, but its spectral bandwidth is limited to the crystal carrier frequency, and the generated THz radiation will usually be strongly absorbed by the water during the propagation, therefore its application is greatly restricted. Recently, as an alternative approach, the two-color laser field has been proposed to generate the intense and broadband THz pulse.[7,13–24] In this two-color laser field scheme, a fundamental femtosecond laser field combining with its second harmonic field is focused in air to generate gaseous plasma, which can deliver a THz pulse with its field intensity higher than 100 MV/m over the spectral width of 100 THz.[25] Furthermore, the plasma-THz generation and detection can be closed to the target,[26,27] which can avoid the attenuation of THz radiation in the air, and thus makes THz remote sensing and other potential applications become possible. Consequently, this plasma-based THz generation technique has aroused a great deal of interest in the past decade.

In the conventional two-color laser field setup, the 800 nm fundamental laser and its harmonic laser are usually employed to generate the THz pulse in the air. Recently, several studies have demonstrated that the THz pulse intensity can be further increased by using the longer wavelength lasers,[28–31] and the recent report showed that a near 30-fold enhancement of THz radiation can be realized by the 1800 nm laser compared to the traditional 800 nm laser.[28] Thus, the use of the near-IR and even mid-IR pump lasers to increase the THz radiation intensity becomes the focus in the high-field THz studies. In those studies, the THz enhancement is mainly attributed to the wavelength-dependence plasma current, so the analysis is still relatively rough and needs to be further refined. Since the plasma current is essentially determined by the stepwise increase of the free electron density and electron drift velocity, the two parameters are sensitive to the waveform of the optical field. When the laser wavelength increases, the optical cycle will decrease under the same laser pulse duration, and the waveform of the laser pulse will be changed, which

*Project supported by the National Natural Science Foundation of China (Grant Nos. 51132004, 11604205, and 11474096), Science and Technology Commission of Shanghai Municipality, China (Grant No. 14JC1401500), Shanghai Municipal Education Commission, China (Grant No. ZZGCD15066), and Foundation of Fujian Educational Committee, China (Grant No. JAT160412).

†Corresponding author. E-mail: lchhuiz@163.com

‡Corresponding author. E-mail: sazhang@phy.ecnu.edu.cn

© 2017 Chinese Physical Society and IOP Publishing Ltd

will affect the above two parameters, and finally determine the THz radiation intensity. Therefore, the effect of the two-color laser wavelength on the THz radiation intensity can be further explained from this microscopic aspect.

In this paper, we study the laser wavelength effect on the intense THz generation in the two-color laser field scheme based on a transient photocurrent model. We show that the THz amplitude increases as the laser wavelength increases at given laser intensity and duration, which is consistent with the previous experimental and theoretical results.[28–31] Furthermore, the enhancement mechanism is explained by using a local current approximation. Our analysis shows that the ionization events play an important role in THz generation, and are sensitive to the change of the laser wavelength. With the increase of the two-color laser wavelength, the number of corresponding ionization events decreases, but the induced electron density in each ionization event will increase, and thus the total electron density keeps a constant. Moreover, we demonstrate that the electron drift velocity is proportional to the laser wavelength for each ionization event, which means that the electron production concentrates in a few ionization events and obtains a higher velocity for the laser with a long wavelength. Hence, the intense plasma current can be generated by the long wavelength laser excitation, and emit the high-field THz pulse.

2. Theoretical model

Our theoretical simulation is based on a transient photocurrent model.[7,14] Here, the employed two-color laser field is a superposition of the fundamental laser field and its second harmonic field, which can be expressed as

$$E(t)=\exp\left(-2\ln 2t^2/\tau^2\right)\left[E_1\cos\omega_0 t+E_2\cos(2\omega_0 t+\phi)\right], \quad (1)$$

where E_1 and E_2 are the amplitudes of the fundamental laser field and its second harmonic field, respectively, τ is the pulse duration, ω_0 is the central frequency of the fundamental laser field, and ϕ is the relative phase between the fundamental laser field and its second harmonic field. Here, the well-known static tunneling model is employed,[20,32] and therefore the ionization rate can be written as

$$W_{\mathrm{ST}}=\frac{\alpha_{\mathrm{ST}}}{|\varepsilon(t)|}\exp\left[-\left(\frac{\beta_{\mathrm{ST}}}{\varepsilon(t)}\right)\right], \quad (2)$$

where $\varepsilon(t)=E(t)/\varepsilon_{\mathrm{a}}$, ε_{a} is the electric field in atomic unit, $\alpha_{\mathrm{ST}}=4\omega_{\mathrm{a}}\gamma_{\mathrm{H}}^{5/2}$, and $\beta_{\mathrm{ST}}=(2/3)\gamma_{\mathrm{H}}^{3/2}$. ω_{a} is the atomic frequency unit with $\omega_{\mathrm{a}}=\kappa^2 me^4/\hbar^3\approx 4.13\times 1016$ S^{-1}, γ_{H} is the ionization potential of the gaseous molecule relative to hydrogen atom with $\gamma_{\mathrm{H}}=U_{\mathrm{ion}}/U_{\mathrm{ion}}^{\mathrm{H}}$. In our simulation, we use $U_{\mathrm{ion}}=15.6$ eV (for N_2 gas) and $U_{\mathrm{ion}}^{\mathrm{H}}=13.6$ eV. Given the ionization rate W_{ST}, the increasing rate of the electron density can be obtained as

$$\frac{\mathrm{d}N_{\mathrm{e}}(t)}{\mathrm{d}t}=W_{\mathrm{ST}}[N_{\mathrm{g}}-N_{\mathrm{e}}(t)], \quad (3)$$

where $N_{\mathrm{e}}(t)$ is the time-dependent electron density and N_{g} is the initial neutral gas density. Furthermore, we use the final ionization degree W_{fi} as a measurement of the electron density, which is written as

$$W_{\mathrm{fi}}=N_{\mathrm{e}}(t=\infty)/N_{\mathrm{g}}, \quad (4)$$

with $W_{\mathrm{fi}}=1$ for the complete ionization. Once the electron is freed from the parent molecule, it will oscillate with the laser field. Thus, the electron velocity at a subsequent time can be written as

$$v(t,t')=-\frac{e}{m}\int_{t'}^{t}E(t'')\,\mathrm{d}t'', \quad (5)$$

where t' is the time when the electron is released. The initial velocity of the electron is assumed to be zero. Considering the contribution of all ionized electrons, the generated transverse electron current can be expressed as

$$J(t)=\int_{t_0}^{t}ev(t,t')\exp[-(t-t')/\gamma]\,\mathrm{d}N_{\mathrm{e}}(t'), \quad (6)$$

where $\mathrm{d}N_{\mathrm{e}}(t')$ represents the change of the electron density in the interval between t and t', $v(t,t')$ is the velocity of these electrons at time t, and γ is the phenomenological electron–ion collision rate ($\gamma=5$ ps^{-1} at atmospheric pressure).[29] The time evolving electron current $J(t)$ can generate the electromagnetic pulse at THz frequency in the far field, and the amplitude of the THz field is proportional to the derivation of electron current $J(t)$ and written as

$$E_{\mathrm{THz}}\propto\frac{\mathrm{d}}{\mathrm{d}t}[J(t)]. \quad (7)$$

Finally, the THz radiation spectrum $E_{\mathrm{THz}}(\omega)$ is obtained by the Fourier transform of E_{THz}(t), i.e., $E_{\mathrm{THz}}(\omega)=\mathrm{FFT}[E_{\mathrm{THz}}(t)]$. In our simulation, the total laser intensity of the two-color laser field is set to be $I_{\mathrm{total}}=200$ TW/cm^2, the pulse duration $\tau=50$ fs, the relative intensity ratio and phase of the two laser fields are $R=I_{2\omega}/I_{\omega}=0.2$ and $\phi=0.5\pi$, respectively, and ω_0 and λ_0 represent the central frequency and wavelength of the fundamental laser field, respectively.

3. Results and discussion

Figure 1 shows the time-dependent electron current $J(t)$ and its corresponding THz radiation spectrum $E_{\mathrm{THz}}(\omega)$ with the laser wavelengths $\lambda_0=400$ nm (black line), 800 nm (red line), and 1600 nm (green line). As can be seen in Fig. 1(a), the electron current $J(t)$ is asymmetrically distributed, and a quasi-DC current arises after the laser pulse. This current surge occurs in the time scale of photoionization process (<100 fs in the general case), which leads to the generation of intense and broadband electromagnetic radiation at THz frequency. As can be seen in Fig. 1(b), the THz radiation has a broad spectral range up to 50 THz. More importantly, it can

be seen in Fig. 1 that both the electron current and the corresponding THz amplitude obtain the maximal values at the laser wavelength $\lambda_0 = 1600$ nm for the given total laser intensity of $I_{\text{total}} = 200$ TW/cm^2 and pulse duration of $\tau = 50$ fs. In other words, using the near- or mid-IR laser can enhance the intensity of THz radiation under the same laser intensity and pulse duration. The results in Fig. 1 also show that the electron current calculation is very useful to investigate the effects of the laser parameters on the THz generation since it can estimate the ultimate current intensity after the laser pulse passage. However, this calculation cannot completely illustrate the physical mechanism since the electron production and motion occur in the sub-femtosecond scale. Therefore, here we use a local current (LC) approximation to further study the THz generation at different laser wavelengths, which can analyze the electron production and motion from a more microscopic aspect.[17,18,30,32]

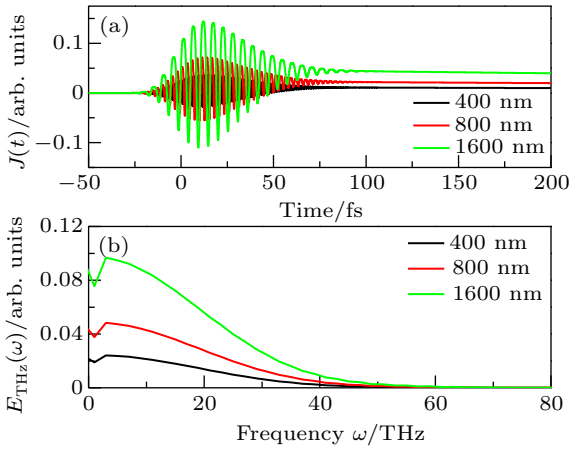


Fig. 1. (color online) The time-varying electron currents $J(t)$ with the laser wavelengths $\lambda_0 = 400$ nm (black line), 800 nm (red line), and 1600 nm (green line) for the given total laser intensity of $I_{\text{total}} = 200$ TW/cm^2 and pulse duration of $\tau = 50$ fs. This current surge gives rise to the electromagnetic radiation, and the corresponding THz radiation spectrum (b) can be obtained from the Fourier transform $\frac{\mathrm{d}}{\mathrm{d}t}[J(t)]$ and low-pass filter.

In the LC model, the time-varying electron current $J(t)$ can be decomposed into two components $J_{\text{A}}(t)$ and $J_{\text{B}}(t)$.[30] The former mainly contains the high frequency pump spectrum, and the later contains the THz spectrum related to the ionization events at time $t = t_n$. These ionization events only occur near the extreme of the two-color laser field at time t_n and correspond to the stepwise increase of the electron density in attosecond-scale, which are sensitive to the waveform of the laser pulse. Thus, we can compare these ionization events at different laser wavelengths, and illustrate the plasma-THz generation from the microscopic aspect and finally estimate the THz radiation amplitude. Usually, these ionization events are well separated from each other, and thus the electron density and current can be written as a sum over the contributions from all the ionization events[30,32]

$$\rho(t) = \sum_n \delta\rho_n H(t - t_n), \tag{8}$$

$$J_{\text{B}}(t) = \sum_n J_n(t) = -\sum_n q\delta\rho_n v_{\text{f}}(t_n) H(t - t_n), \tag{9}$$

where $\delta\rho_n$ and $v_{\text{f}}(t_n)$ represent the electron density and velocity in the n-th ionization event, respectively. Then, the generated THz pulse in the frequency domain can be obtained by the Fourier transform of Eq. (9)

$$E_{\text{THz}}(\omega) \propto \sum_n C_n \mathrm{e}^{\mathrm{i}\omega t_n}, \tag{10}$$

with

$$C_n = q\delta\rho_n v_{\text{f}}(t_n), \tag{11}$$

where C_n represents the amplitude of the n-th attosecond current burst, which is produced around the n-th ionization event and determined by the electron density $\delta\rho_n$ and velocity $v_{\text{f}}(t_n)$. As can be seen in Eq. (10), the THz spectrum is a superposition of contributions from these individual ionization events. Due to the spectral phase $\mathrm{e}^{\mathrm{i}\omega t}$, the contributions from the high frequency components will cancel each other and those from the low frequency components interfere instructively. Finally, the THz spectrum can be obtained, and its amplitude is determined by the total amplitude of the current bursts $C_{\text{total}} = \sum C_n$. Obviously, this model provides a novel approach to predict the THz radiation amplitude, and can also be used to analyze the THz generation from the microscopic aspect.

Figure 2 shows the amplitude of the n-th current burst with the laser wavelengths $\lambda_0 = 400$ nm (black squares), 800 nm (red circles) and 1600 nm (green triangles) for the total laser intensity of $I_{\text{total}} = 200$ TW/cm^2 and pulse duration of $\tau = 50$ fs. As can be seen, the number of ionization events decreases with the increase of the laser wavelength at the fixed duration since the optical cycle decreases for the long wavelength laser. But the amplitude of the single ionization event increases with the increase of the laser wavelength. It can be seen that the amplitude with laser wavelength $\lambda_0 = 1600$ nm is nearly four times of that with laser wavelength $\lambda_0 = 800$ nm, and the same cases can also be observed for the 800 nm and 400 nm lasers. Furthermore, the total amplitude of the current bursts C_{total} also obtains the maximal value at the laser wavelength $\lambda_0 = 1600$ nm among the three laser wavelengths, as shown in the inset of Fig. 2. This result is in good agreement with that of Fig. 1. Only comparing the single ionization events cannot completely illustrate the total amplitude of the current bursts and the corresponding THz radiation intensity, since the total amplitude is determined by all the contributions of the ionization events, while the optical cycle will be changed for different wavelength lasers at the same pulse duration. Fortunately, it can be found that the ionization event occurs once for the 1600 nm laser in its half optical period,

and twice within this period for the 800 nm laser since the optical period of the 800 nm laser is half of that of the 1600 nm laser, but the sum of the two ionization event amplitudes by the 800 nm laser is also lower than that of once by the 1600 nm laser. Thus, we can analyze the amplitude of current bursts in the short time interval to illustrate the THz radiation enhancement mechanism.

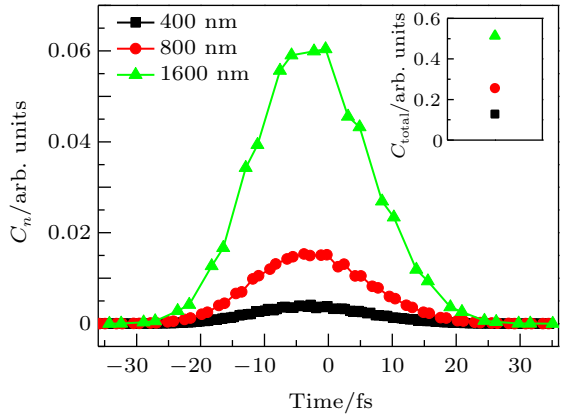


Fig. 2. (color online) The amplitudes of the n-th current burst C_n with the laser wavelengths $\lambda_0 = 400$ nm (black squares), 800 nm (red circles), and 1600 nm (green triangles) for the given laser intensity of $I_{\rm total} = 200$ TW/cm^2 and pulse duration of $\tau = 50$ fs. The position of these symbols corresponds to the time of the ionization event, and the number increases with the increase of the laser wavelength. Inset shows the total current amplitudes $C_{\rm total}$ for the three wavelength lasers.

Since the amplitude of the n-th current burst C_n is determined by the electron density and velocity, we can discuss the THz generation by analyzing the two parameters in an optical period of the long wavelength laser (i.e., $\lambda_0 = 1600$ nm). We first study the dependence of the electron density on the laser wavelength. Figure 3 shows the time-varying ionization degree $W_{\rm fi}$ with the laser wavelengths $\lambda_0 = 400$ nm (black line), 800 nm (red line), and 1600 nm (blue line) for the given total laser intensity $I_{\rm total} = 200$ TW/cm^2 and pulse duration $\tau = 50$ fs. As can be seen, the free electron density shows a stepwise increase process in a short-attosecond scale, and the final electron density approaches the same value after the laser pulse passage for the three laser wavelengths. It means that the final electron density depends on the laser intensity and pulse duration, but is not related to the laser wavelength. This conclusion is also valid in the short time interval. The inset of Fig. 3 shows the time varying ionization degree $W_{\rm fi}$ in an optical period of the 1600 nm laser. As can be seen, the ionization event occurs twice for the 1600 nm laser, and the corresponding electron density jumps twice in this time interval, but the ionization event for the 800 nm laser occurs four times, and therefore the electron density jumps four times. Although the number of the ionization events is different, the increase of the electron density is almost the same in such a time interval. The result can be further explained by the LC current model. In this model, the increase of the electron density for the n-th ionization event is expressed as[30]

$$\delta\rho_n = \rho_0\, \mathrm{e}^{-\sum_{j=1}^{n-1}\sqrt{\pi}\tau_j W(|E(t_j)|)}\left(1-\mathrm{e}^{-\sqrt{\pi}\tau_n W(|E(t_n)|)}\right), \quad (12)$$

where τ_n is the duration of the n-th ionization event, ρ_0 is the density of neutral atoms, and $W[|E(t_n)|]$ is the instantaneous tunnel ionization rate. In the one optical period of the 1600 nm laser, the ionization event occurs twice, and the increase of the electron density is given by

$$\rho_{1600}(\Delta t) = \delta\rho_1 + \delta\rho_2. \quad (13)$$

In the same time interval, the ionization event occurs four times for the 800 nm laser, and the corresponding increase of the electron density is written as

$$\rho_{800}(\Delta t) = \delta\rho_1' + \delta\rho_2' + \delta\rho_3' + \delta\rho_4'. \quad (14)$$

By using some approximations (see Appendix A), one can obtain the relationship

$$\delta\rho_1 + \delta\rho_2 \approx \delta\rho_1' + \delta\rho_2' + \delta\rho_3' + \delta\rho_4'. \quad (15)$$

This result further proves that the increase of the electron density is almost the same, which is independent of the laser wavelength. It is very helpful for comparing the amplitude of the ionization events in a fixed short time interval.

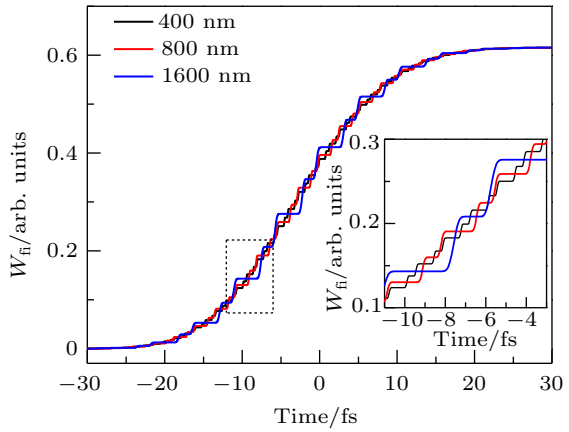


Fig. 3. (color online) The time-varying ionization degrees $W_{\rm fi}$ with the laser wavelengths $\lambda_0 = 400$ nm (black line), 800 nm (red line), and 1600 nm (blue line) for the given laser intensity of $I_{\rm total} = 200$ TW/cm^2 and pulse duration of $\tau = 50$ fs. The electron density reaches the same saturation after the laser pulse passage. Inset shows the time-varying ionization degrees $W_{\rm fi}$ in an optical period of 1600 nm laser for the three wavelength lasers. In the short time interval, the electron density jumps twice for the 1600 nm laser but four times for the 800 nm laser.

Figure 4 shows the electron velocity $v_{\rm f}(t_n)$ with the laser wavelengths $\lambda_0 = 400$ nm (black squares), 800 nm (red circles), and 1600 nm (green triangles) for the total laser intensity $I_{\rm total} = 200$ TW/cm^2. As can be seen, the number of ionization events decreases with the increase of the laser wavelength. It means that the electron production and movement occur in a fewer moments for the long wavelength laser. Furthermore, in the same ionization time, the electron velocity increases with the increase of the laser wavelength, and the electron velocity for the 1600 nm laser is nearly twice of that for the 800 nm

laser. Consequently, it can be speculated that the electron velocity is related to the laser wavelength. Next, we further demonstrate this relationship. After introducing the two-color electric field in Eq. (1) into the electron velocity in Eq. (5), we can obtain (see Appendix B)

$$v_{\rm f}(t_n) = \frac{q}{m\omega_0} {\rm e}^{-2\ln 2 t_n^2/\tau^2} \left(E_1 \sin \omega_0 t_n + \frac{1}{2} E_2 \sin 2\omega_0 t_n \right). \quad (16)$$

In the above equation, the two items in the bracket correspond to the oscillation of the two different color laser fields. The change of the laser frequency ω_0 mainly increases or decreases the optical cycle, and finally affects the number of the ionization events. However, in the same ionization time t_n, the amplitude of the electron velocity is proportional to the laser wavelength, which is given by

$$|v_{\rm f}(t_n)| \propto \frac{1}{\omega_0} \propto \lambda_0. \quad (17)$$

Obviously, the analysis is consistent with the result in Fig. 4. As can be seen, the ionization event number decreases with the increase of the laser wavelength, but the amplitude of the electron velocity increases.

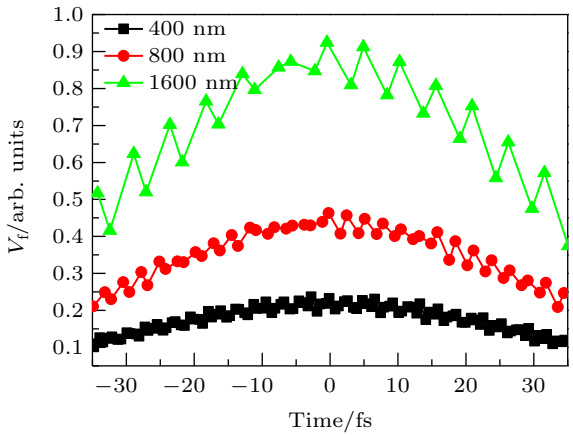


Fig. 4. (color online) The electron velocities $V_{\rm f}$ with the laser wavelengths $\lambda_0 = 400$ nm (black squares), 800 nm (red circles), and 1600 nm (green triangles) for the given laser intensity of $I_{\rm total} = 200$ TW/cm^2 and pulse duration of $\tau = 50$ fs. The positon of the symbols corresponds to the ionization event, and its value represents the velocities of electron produced in the ionization events.

Based on the above discussion, we compare the amplitudes of the ionization events in an optical period of the 1600 nm laser. In this time interval, the ionization event occurs twice for the 1600 nm laser, and the amplitude of the ionization events can be expressed as

$$C_{1600} = \delta\rho_1 v_{\rm f}(t_1) + \delta\rho_2 v_{\rm f}(t_2), \quad (18)$$

where t_i $(i = 1, 2)$ represent the ionization time of the two ionization events for the 1600 nm laser, respectively. In this time interval, the ionization event occurs four times for the 800 nm laser, and the amplitude of the ionization events can be expressed as

$$C_{800} = \delta\rho_1' v_{\rm f}(t_1') + \delta\rho_2' v_{\rm f}(t_2') + \delta\rho_3' v_{\rm f}(t_3') + \delta\rho_4' v_{\rm f}(t_4'), \quad (19)$$

where t_i' $(i = 1$–$4)$ represent the ionization time of the four ionization events for the 800 nm laser, respectively. On the basis of the above analysis, we have

$$\delta\rho_1 \approx \delta\rho_1' + \delta\rho_2', \quad \delta\rho_2 \approx \delta\rho_3' + \delta\rho_4', \quad (20)$$

$$v_{\rm f}(t_1) \approx 2v_{\rm f}(t_1') \approx 2v_{\rm f}(t_2'), \quad v_{\rm f}(t_2) \approx 2v_{\rm f}(t_3') \approx 2v_{\rm f}(t_4'), \quad (21)$$

$$C_{1600} \approx 2C_{800} = \frac{\lambda_{1600}}{\lambda_{800}} C_{800}. \quad (22)$$

As can be seen, the amplitude of the current burst for the 1600 nm laser is two times of that for the 800 nm laser. It is obvious that the amplitude ratio is equal to the laser wavelength ratio. Considering all the contributions of the ionization events in the whole pulse duration, the total amplitude of the current bursts $C_{\rm total}$ should have the same relationship. These results can also be seen in Fig. 2 and its inset. Consequently, the amplitude of the THz radiation is linearly dependent on the laser wavelength, and this conclusion coincides with the previous report.[28,31] In particular, the total electron density is independent of the laser wavelength, but the electron velocity depends on the laser wavelength, and the longer wavelength laser can stimulate the larger electron velocity. Since the THz amplitude depends on both the electron density and the velocity of each ionization event, the THz radiation can be stronger with the longer wavelength laser. Obviously, the above analysis can well explain the enhancement mechanism of THz radiation for the long wavelength laser.

Finally, we present the dependence of the THz amplitude on the laser wavelength at the given laser intensity of $I_{\rm total} = 200$ TW/cm^2 and pulse duration of $\tau = 50$ fs. The simulated result is shown in Fig. 5. As can be seen, the THz amplitude linearly increases with the increase of the laser wavelength. Moreover, the THz amplitude for the 1600 nm laser is two times of that for the 800 nm pump laser. Such a result further confirms the above analysis, i.e., the THz output is proportional to the laser wavelength $C_{1800} \approx \lambda_{1800}/\lambda_{800} \times C_{800}$. Here, we focus on the scaling law between the pump wavelength and the THz amplitude; this relationship provides a very useful reference to estimate the amplitude of THz pulse by using mid- or far-infrared lasers. Furthermore, considering the real experimental condition, the scaling law between the wavelength and THz energy can be further correct. In the fixed focal length and input energy condition, which combines the effect of the wavelength-dependence plasma volume, the 30 times higher THz energy can be realized at 1800 nm wavelength compared to 800 nm wavelength.[28]

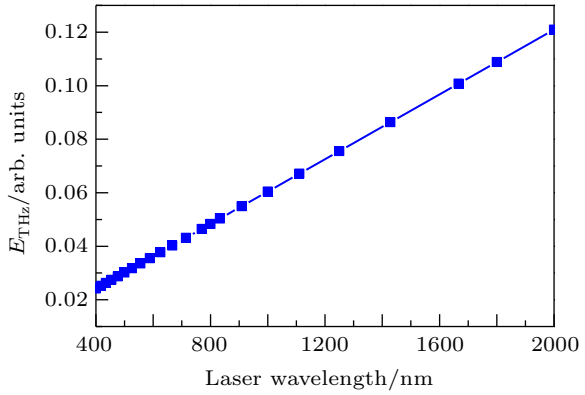


Fig. 5. (color online) The THz amplitude E_{THz} as a function of the laser wavelength λ_0 for the given laser intensity of $I_{\mathrm{total}} = 200$ TW/cm^2 and pulse duration of $\tau = 50$ fs. The THz amplitude increases with the increase of the laser wavelength, which shows a linear relationship.

4. Conclusion

In summary, we have theoretically demonstrated the dependence of THz generation on the two-color laser wavelength based on a transient photocurrent model. Our results showed that the THz amplitude increases with the increase of the laser wavelength for given laser intensity and duration, and the THz amplitude is attributed to the superposition of contributions from the individual ionization events. Furthermore, the enhancement mechanism of the THz radiation for the long wavelength laser was analyzed by using the local current model. It was shown that the THz amplitude depends on both the electron density and velocity of each ionization event, the electron density is independent of the laser wavelength, while the electron velocity depends on the laser wavelength, and the longer wavelength laser can simulate the larger electron velocity, which thus results in the THz radiation enhancement. These theoretical results can provide a feasible scheme to analyze the THz generation process under the two-color laser field, and also will be very useful for further controlling and optimizing the intense THz output.

Appendix A: comparison of electron density

In the LC current model, the increase of the electron density in the n-th ionization event is expressed as[23]

$$\delta\rho_n = \rho_0 \mathrm{e}^{-\sum_{j=1}^{n-1}\sqrt{\pi}\tau_j W(|E(t_j)|)}\left(1-\mathrm{e}^{-\sqrt{\pi}\tau_n W(|E(t_n)|)}\right), \quad \text{(A1)}$$

where τ_n is the duration of the n-th ionization event, ρ_0 is the density of neutral atoms, and $W[|E(t_n)|]$ is the instantaneous tunnel ionization rate. In one period of the 1600 nm laser, the ionization event occurs twice, and thus the increase of the electron density is given by

$$\begin{aligned}\rho_{1600}(\Delta t) &= \delta\rho_1 + \delta\rho_2 \\ &= \rho_0\left(1-\mathrm{e}^{-\sqrt{\pi}\tau_1 W(|E(t_1)|)}\,\mathrm{e}^{-\sqrt{\pi}\tau_2 W(|E(t_2)|)}\right), \quad \text{(A2)}\end{aligned}$$

where t_i and τ_i $(i = 1,2)$ represent the ionization time and duration of the two ionization events for the 1600 nm laser, respectively. In the same time interval, the ionization event occurs four times for the 800 nm laser, and the corresponding increase of the electron density is written as

$$\begin{aligned}\rho_{800}(\Delta t) &= \delta\rho_1' + \delta\rho_2' + \delta\rho_3' + \delta\rho_4' \\ &= \rho_0\left(1-\mathrm{e}^{-\sqrt{\pi}\left(\tau_1' W\left(|E(t_1')|\right)+\tau_2' W\left(|E(t_2')|\right)\right)}\right. \\ &\quad \left.\times\,\mathrm{e}^{-\sqrt{\pi}\left(\tau_3' W\left(|E(t_3')|\right)+\tau_4' W\left(|E(t_4')|\right)\right)}\right), \quad \text{(A3)}\end{aligned}$$

where t_i' and τ_i' $(i = 1$–$4)$ represent the ionization time and duration of the four ionization events for the 800 nm laser, respectively. Since the envelope of the laser pulse slowly changes, and the ionization event only occurs near the extreme of the laser field, thus the electric field in the ionization time is approximately equal, such that

$$E(t_1) \approx E(t_1') \approx E(t_2'), \;\; E(t_2) \approx E(t_3') \approx E(t_4'). \quad \text{(A4)}$$

Furthermore, the duration is related to the laser wavelength, the optical period of the 1600 nm laser is twice of that of the 800 nm laser, thus

$$\tau_1 \approx \tau_1' + \tau_2', \;\; \tau_2 \approx \tau_3' + \tau_4'. \quad \text{(A5)}$$

Finally, we can obtain the approximation

$$\delta\rho_1 + \delta\rho_2 \approx \delta\rho_1' + \delta\rho_2' + \delta\rho_3' + \delta\rho_4'. \quad \text{(A6)}$$

Appendix B: approximation of electron velocity

Substituting the two-color electric field in Eq. (A1) into the electron velocity in Eq. (A5), we can obtain

$$v_{\mathrm{f}}(t_n) = \frac{q}{m}\int_{-\infty}^{t_n} E(t)\,\mathrm{d}t = v_{\mathrm{f1}}(t_n) + v_{\mathrm{f2}}(t_n), \quad \text{(B1)}$$

where

$$v_{\mathrm{f1}}(t_n) = \frac{qE_1}{m}\int_{-\infty}^{t_n} \mathrm{e}^{-2\ln 2t^2/\tau^2}\cos\omega_0 t\,\mathrm{d}t, \quad \text{(B2)}$$

$$v_{\mathrm{f2}}(t_n) = \frac{qE_2}{m}\int_{-\infty}^{t_n} \mathrm{e}^{-2\ln 2t^2/\tau^2}\cos 2\omega_0 t\,\mathrm{d}t, \quad \text{(B3)}$$

$$a = -\frac{2\ln 2}{\tau^2}. \quad \text{(B4)}$$

By the integration of Eq. (B2), we obtain

$$\begin{aligned}v_{\mathrm{f1}}(t_n) = \frac{qE_1}{m}\left[\frac{1}{\omega_0}\mathrm{e}^{at_n^2}\sin\omega_0 t_n + \frac{2a}{\omega_0^2}t_n\mathrm{e}^{at_n}\cos\omega_0 t_n\right. \\ \left.-\frac{2a}{\omega_0^2}\int_{-\infty}^{t_n}(1+2at_n)\,\mathrm{e}^{at^2}\cos\omega_0 t\,\mathrm{d}t\right]. \quad \text{(B5)}\end{aligned}$$

Since the laser pulse has a lot of optical cycles, $1/\omega_0 < \tau$, we can have the approximation

$$\left|\frac{2at_n}{\omega_0^2}\right| = 4\frac{\ln 2}{\omega_0^2\tau^2}t_n \ll 1, \;\; \left|\frac{2a}{\omega_0^2}\right| = 4\frac{\ln 2}{\omega_0^2\tau^2} \ll 1. \quad \text{(B6)}$$

Thus, the second and the third items in the bracket of Eq. (B5) can be neglected, and therefore it can be further simplified as

$$v_{\mathrm{f1}}(t_n) == \frac{qE_1}{m\omega_0}\,\mathrm{e}^{at_n^2}\sin\omega_0 t_n. \tag{B7}$$

Similarly, equation (B3) can also be simplified with the same approximation, and finally the electron velocity in Eq. (B1) can be written as

$$v_{\mathrm{f}}(t_n) = \frac{q}{m\omega_0}\,\mathrm{e}^{-2\ln 2t_n^2/\tau^2}\left(E_1\sin\omega_0 t_n + \frac{1}{2}E_2\sin 2\omega_0 t_n\right). \tag{B8}$$

References

[1] Davies A G, Burnett A D, Fan W, Linfield E H and Cunningham J E 2008 *Materials Today* **11** 18
[2] Han P Y, Cho G C and Zhang X C 2000 *Opt. Lett.* **25** 242
[3] Kleine-Ostmann T and Nagatsuma T 2011 *J. Infrared. Milli. Terahertz Waves* **32** 143
[4] Song H J and Nagatsuma T 2011 *IEEE Tran. Terahertz Sci. Tech.* **1** 256
[5] Johnson J L, Dorney T D and Mittleman D M 2001 *Appl. Phys. Lett.* **78** 835
[6] Liu J, Dai J, Chin S L and Zhang X C 2010 *Nat. Photon.* **4** 627
[7] Kim K Y, Glownia J H, Taylor A J and Rodriguez G 2007 *Opt. Express* **15** 4577
[8] Roskos H G, Thomson M D, Kreß M and Löffler T 2007 *Laser Photonics Rev.* **1** 349
[9] Gildenburge V B and Vvedenskii N V 2007 *Phys. Rev. Lett.* **98** 245002
[10] Auston D H and Smith P R 1983 *Appl. Phys. Lett.* **43** 631
[11] Fattinger and Grischkowsky D 1989 *Appl. Phys. Lett.* **54** 490
[12] Auston H, Cheung K P, Valdmanis J A and Kleinman D A 1984 *Phys. Rev. Lett.* **53** 1555
[13] Cook D J and Hochstrasser R M 2000 *Opt. Lett.* **25** 1210
[14] Kim K Y 2009 *Phys. Plasmas* **16** 056706
[15] Xie X, Dai J and Zhang X C 2006 *Phys. Rev. Lett.* **96** 075005
[16] Kim K Y, Taylor A J, Glownia J H and Rodriguez G 2008 *Nat. Photon.* **2** 605
[17] Babushkin I, Kuehn W, Köhler C, Skupin S, BergéL, Reimann K, Woerner M, Herrmann J and Elsaesser T 2010 *Phys. Rev. Lett.* **105** 53903
[18] Bergé L, Skupin S, Köhler C, Babushkin I and Herrmann J 2013 *Phys. Rev. Lett.* **110** 073901
[19] Silaev A A and Vvedenskii N V 2009 *Phys. Rev. Lett.* **102** 115005
[20] Vvedenskii N V, Korytin A I, Kostin V A, Murzanev A A, Silaev A A and Stepanov A N 2014 *Phys. Rev. Lett.* **112** 055004
[21] Dai H and Liu J 2011 *J. Mod. Opt.* **58** 859
[22] Lu C, He T, Zhang L, Zhang H, Yao Y, Li S and Zhang S 2015 *Phys. Rev. A* **92** 063850
[23] Bai Y, Song L Y, Liu P and Li R X 2017 *Chin. Phys. Lett.* **34** 014201
[24] Li M, Li A Y, He B Q, Yuan S and Zeng H P 2016 *Chin. Phys. B* **25** 044209
[25] Sell A, Leitenstorfer A and Huber R 2008 *Opt. Lett.* **33** 2767
[26] Wang T J, Daigle J F, Yuan S, Théberge F, Châteauneuf M, Dubois J, Roy G, Zeng H and Chin S L 2011 *Phys. Rev. A* **83** 053801
[27] Daigle J F, Théberge F, Henriksson M, Wang T J, Yuan S, Châteauneuf M, Dubois J, Piché M and Chin S L 2012 *Opt. Express* **20** 6825
[28] Clerici M, Peccianti M, Schmidt B E, Caspani L, Caspani L, Shalaby M, Giguère M, Lotti A, Couairon A, Légaré F, Ozaki T, Faccio D and Morandotti R 2013 *Phys. Rev. Lett.* **110** 253901
[29] Vvedenskii N V, Korytin A I, Kostin V A, Murzanev A A, Silaev A A and Stepanov A N 2014 *Phys. Rev. Lett.* **112** 055004
[30] González de Alaiza Martinez P, Babushkin I, Bergé L, Skupin S, Cabrera-Granado E and Kohler C 2015 *Phys. Rev. Lett.* **114** 183901
[31] Wu S, Liu J, Wang S and Zeng Y 2013 *Chin. Opt. Lett.* **11** 101402
[32] Babushkin I, Skupin S, Husakou A, Köhler C, Cabrera-Granado E, Berge L and Herrmann J 2011 *New J. Phys.* **13** 123029